



King's Research Portal

[Link to publication record in King's Research Portal](#)

Citation for published version (APA):

Romeo, S., Secco, I., Schneider, E., Reumiller, C. M., Santos, C. X. C., Zoccarato, A., Musale, V., Pooni, A., Yin, X., Theofilatos, K., Cellone Trevelin, S., Zeng, L., Mann, G., Pathak, V., Harkin, K., Stitt, A. W., Medina, R. J., Margariti, A., Mayr, M., ... Zampetaki, A. (in press). Human blood vessel organoids reveal a critical role for CTGF in maintaining microvascular integrity. *Nature Communications*.

Citing this paper

Please note that where the full-text provided on King's Research Portal is the Author Accepted Manuscript or Post-Print version this may differ from the final Published version. If citing, it is advised that you check and use the publisher's definitive version for pagination, volume/issue, and date of publication details. And where the final published version is provided on the Research Portal, if citing you are again advised to check the publisher's website for any subsequent corrections.

General rights

Copyright and moral rights for the publications made accessible in the Research Portal are retained by the authors and/or other copyright owners and it is a condition of accessing publications that users recognize and abide by the legal requirements associated with these rights.

- Users may download and print one copy of any publication from the Research Portal for the purpose of private study or research.
- You may not further distribute the material or use it for any profit-making activity or commercial gain
- You may freely distribute the URL identifying the publication in the Research Portal

Take down policy

If you believe that this document breaches copyright please contact librarypure@kcl.ac.uk providing details, and we will remove access to the work immediately and investigate your claim.

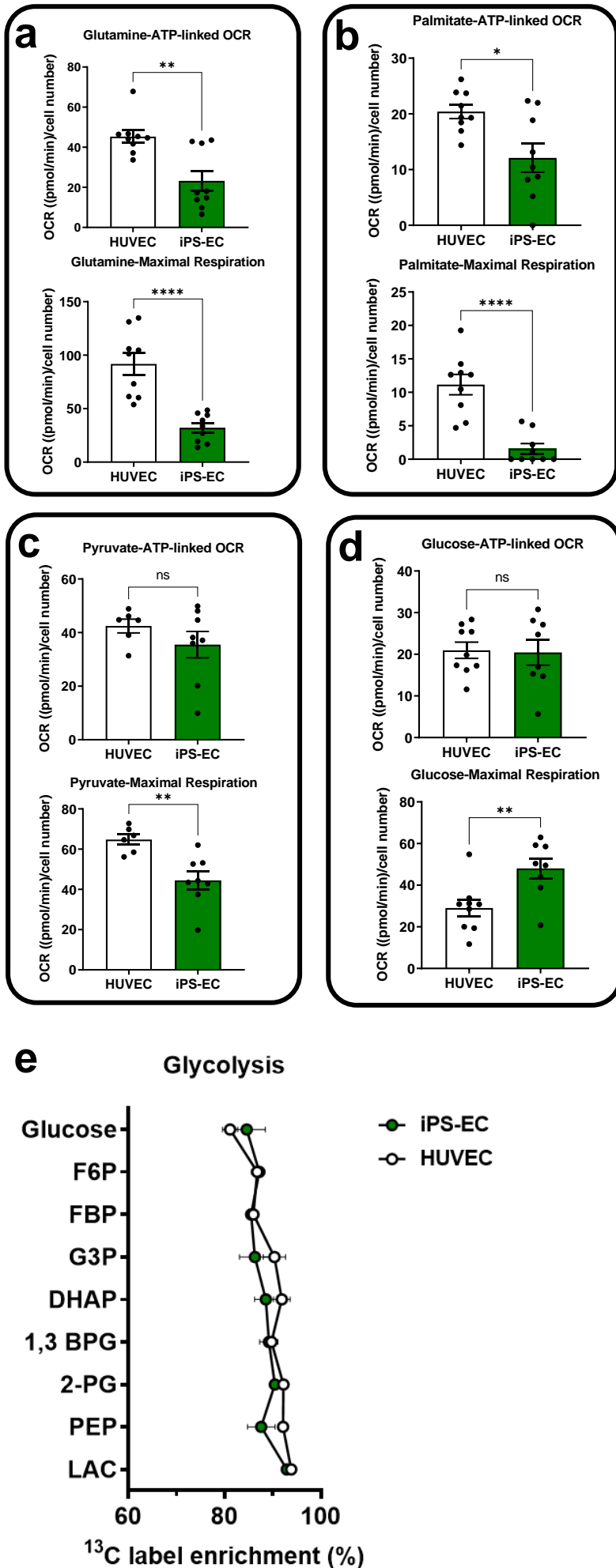
Supplementary Material

Human blood vessel organoids reveal a critical role for CTGF in maintaining microvascular integrity

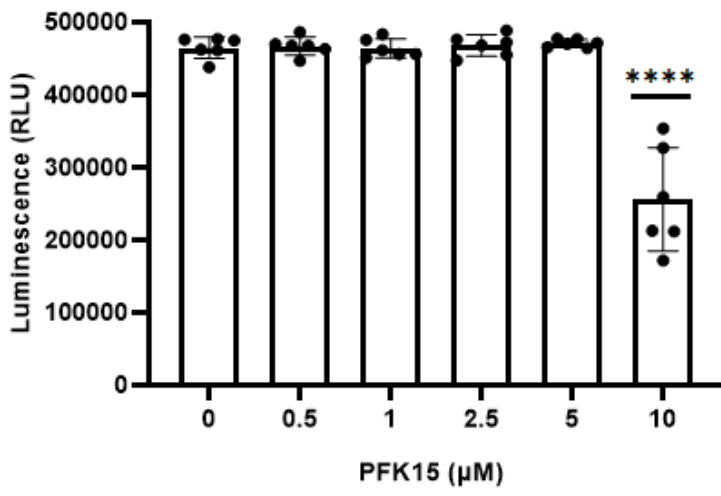
Sara G Romeo¹, Ilaria Secco¹, Edoardo Schneider¹, Christina M Reumiller¹, Celio XC Santos¹, Anna Zoccarato¹, Vishal Musale¹, Aman Pooni¹, Xiaoke Yin¹, Konstantinos Theofilatos¹, Silvia Cellone Trevelin¹, Lingfang Zeng¹, Giovanni E Mann¹, Varun Pathak², Kevin Harkin², Alan W Stitt², Reinhold J Medina², Andriana Margariti², Manuel Mayr¹, Ajay M Shah¹, Mauro Giacca¹ and Anna Zampetaki^{1*}

¹King's College London British Heart Foundation Centre, School of Cardiovascular & Metabolic Medicine and Sciences, London, United Kingdom; ² The Wellcome-Wolfson Institute for Experimental Medicine, Queen's University Belfast, Belfast, United Kingdom.

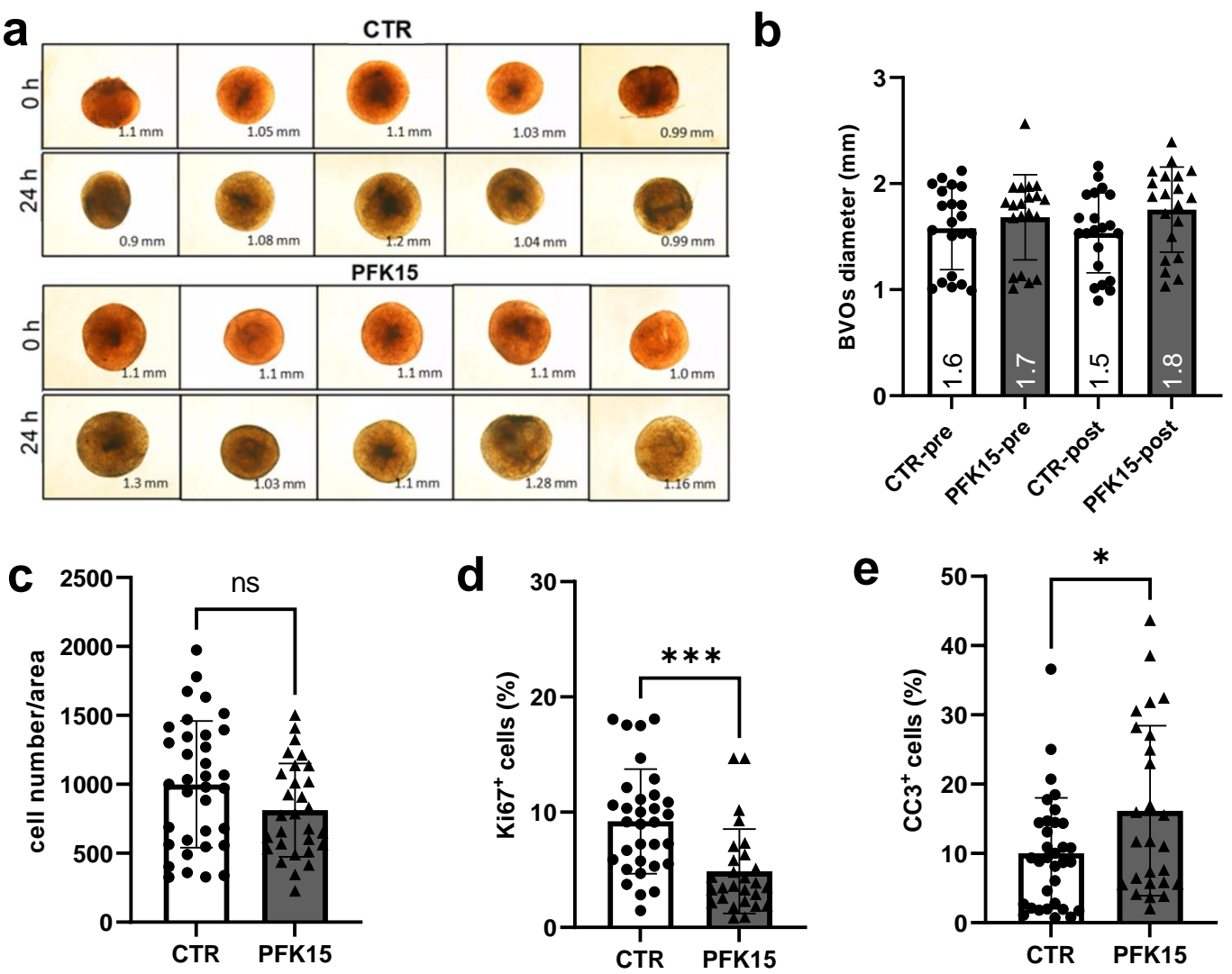
***Corresponding author:** Dr Anna Zampetaki, School of Cardiovascular & Metabolic Medicine and Sciences, James Black Centre, 125 Coldharbour Lane, London SE5 9NU, UK. Email: anna.zampetaki@kcl.ac.uk



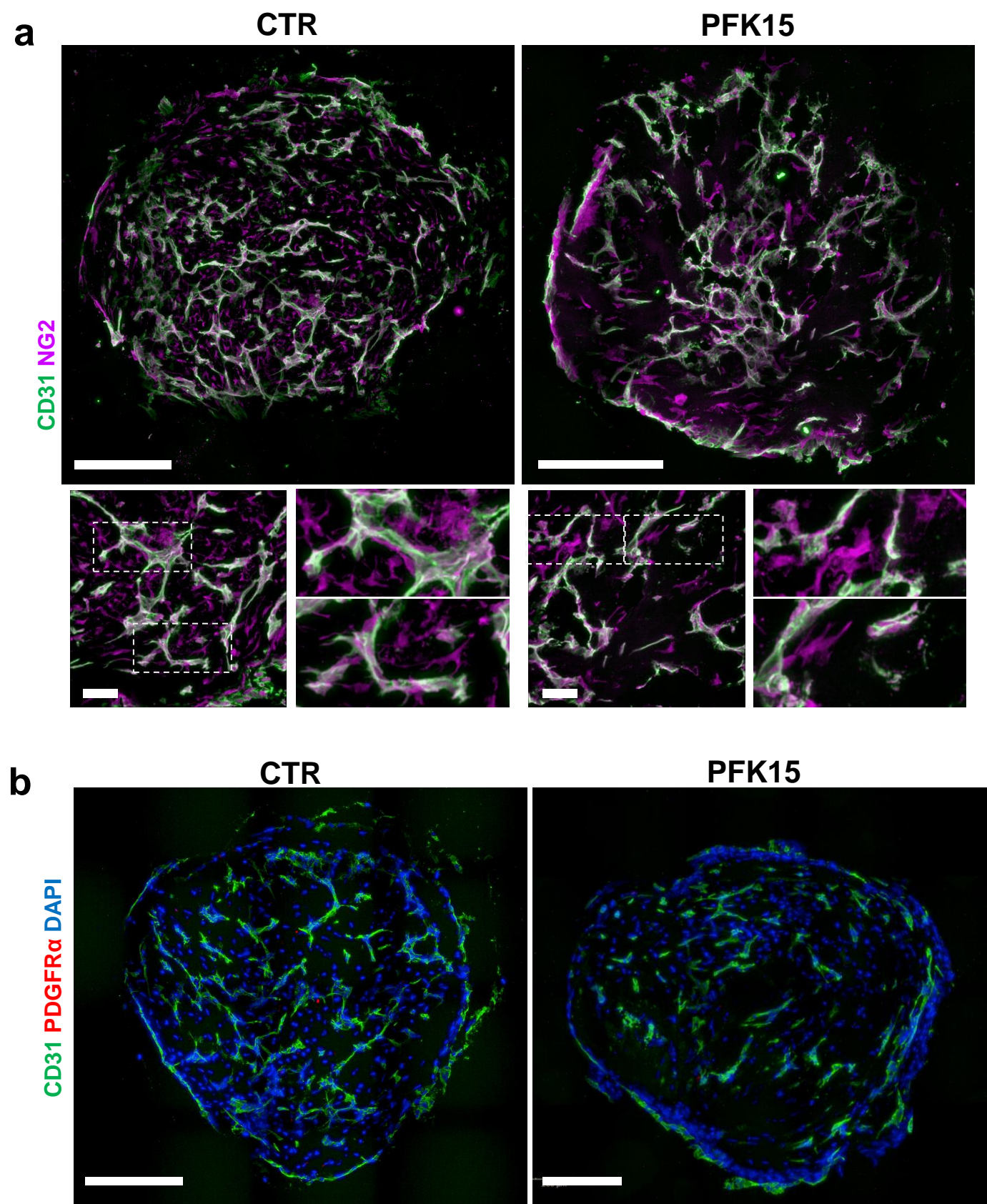
Supplementary Figure 1. Substrate utilisation in iPS-ECs and HUVEC as assessed by Seahorse assays. (a) glutamine, (b) palmitate, (c) pyruvate, (d) glucose, ATP-linked OCR and maximum respiration are shown. Three independent lines were assessed in n=3 wells per assay. Values are presented as mean \pm SEM; P values were calculated using a two-tailed Student's t-test. (a: **p=0.0019; ****p=0.000064; b: *p=0.0101; ****p=0.000038; c: **p=0.0037; d: **p=0.0083). ns= not significant. OCR (Oxygen Consumption Rate). (e) ¹³C label incorporation into glycolytic intermediates in HUVEC and iPS-EC cell lines at baseline after 7h of incubation with ¹³C₆-glucose. Data represents mean \pm SEM, n=3, independent experiments for iPS-ECs and n=4, independent experiments for HUVEC statistical significance was assessed by a two-way ANOVA with Holm-Sidak post-hoc test, Abbreviations: F6P (fructose 6-phosphate). FBP (fructose 1,6-bisphosphate), G3P (Glyceraldehyde 3-phosphate), DHAP (Dihydroxyacetone phosphate), 1,3-BPG (1,3-bisphosphoglycerate), 2-PG (2-phosphoglycerate), PEP (phosphoenolpyruvate), LAC (Lactate).



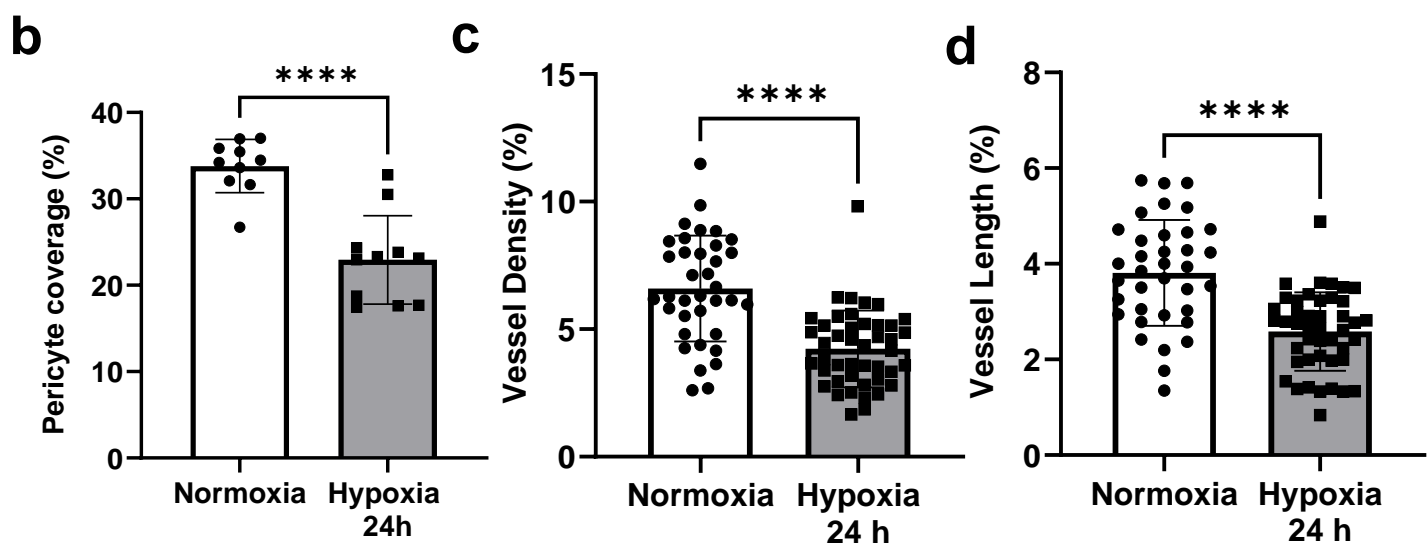
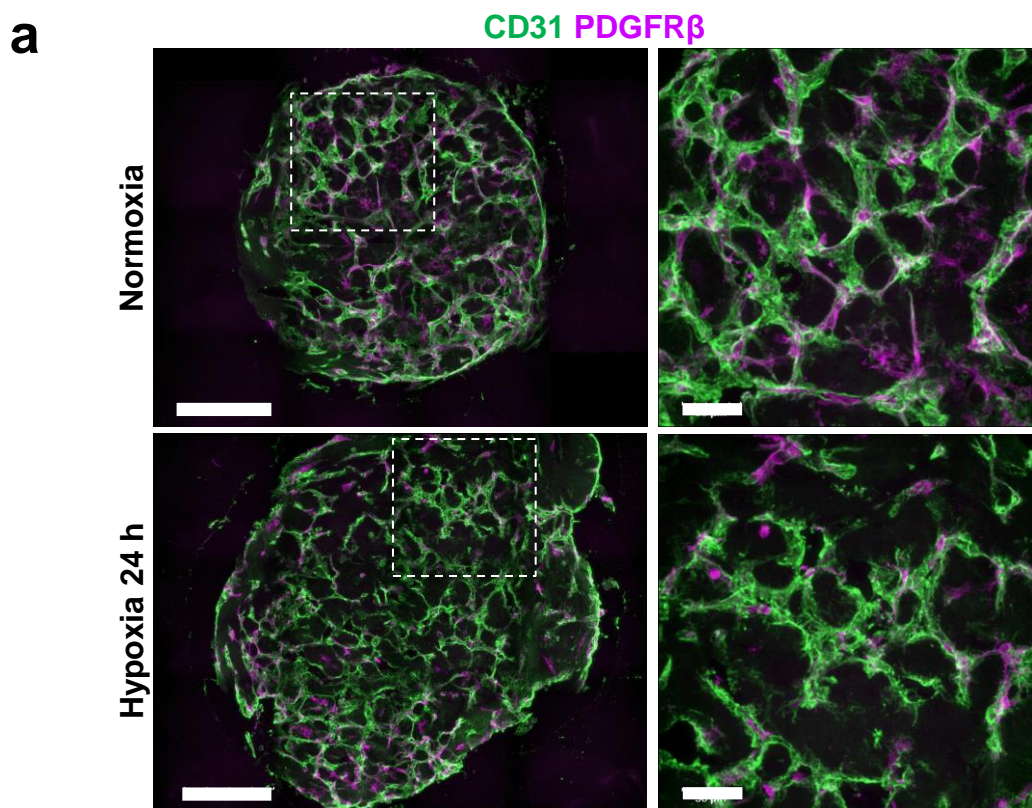
Supplementary Figure 2. Survival of iPS-ECs treated with various concentrations of PFK15 for 24h. Values are presented as mean \pm SD; P values were calculated using one-way ANOVA followed by Tukey's multiple comparisons tests (**** $p=0.000000000000420$) $n=2$ independent experiments.



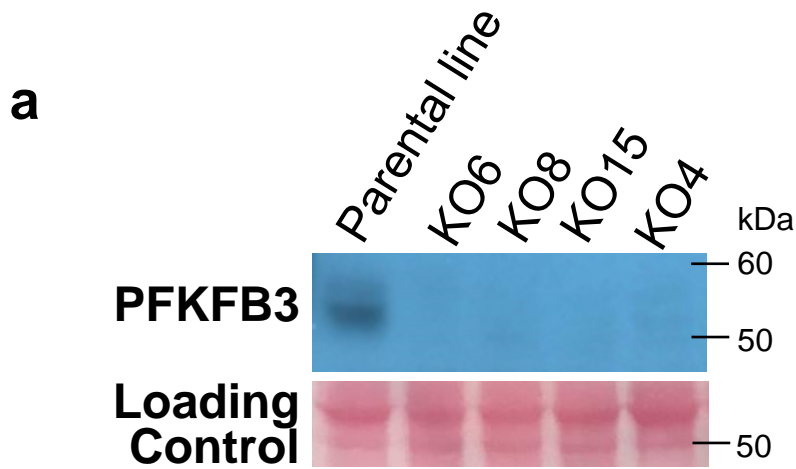
Supplementary Figure 3. The effect of PFK15 on BVO diameter and cellular composition. (a) Bright-field images of BVOs treated with DMSO (CTR) or PFK15 (2.5 μ M) for 24h and (b) quantification of BVO diameter pre- and post-treatment n=20 BVOs per group. (c) Total number of cells per area, (d) percentage of proliferating cells, and (e) percentage of cleaved caspase 3 (CC3) positive cells in n=15 BVOs per group from 5 separate preparations. One-two sections per BVO were assessed. Values are presented as mean \pm SD; P values were calculated using a two-tailed Student's t-test. (d: ***p=0.0002; e: *p=0.0237). ns= not significant.



Supplementary Figure 4. NG2 expression in BVOs following PFK15 treatment. Phenotypic characterization of **(a)** NG2 (magenta) and **(b)** PDGFR α (red) expression in BVO sections using immunofluorescence confocal microscopy. CD31⁺ ECs are shown in green. DAPI is shown in blue. N=5, representative images of 5 independent experiments. Bar scales 200 μ m and 50 μ m.



Supplementary Figure 5. BVOs' structure under hypoxia. (a) Immunofluorescence confocal imaging showing CD31⁺ ECs (green) in vascular networks covered by pericytes (PDGFR β ⁺, magenta) in sections from BVOs under normoxia or hypoxia condition for 24hs. (b) pericyte coverage, n=6 BVOs per group, from 3 separate BVO preparations. One or two sections per BVO were assessed. (c) quantification of vessel density and (d) vessel length. N=6 BVOs per group, from 3 separate BVO preparations and 4 different areas per 10x images have been used for quantification. One or two sections per BVO were assessed. Data are shown as mean \pm SD a two-tailed Student's t-test. (b: ****p=0.000013; c: ****p=0.00000095; d: ****p=0.000000199). Bar scales 200 μ m (left) and 50 μ m (right).



b

PFKFB3 KO6 allele-1 **CCCCC**^{1bp insertion}**ACCGT**_t**CATCGTCATGGTGGGCCTCCCCGCC**

PFKFB3 genome **CCCCC****ACCGT.CATCGTCATGGTGGGCCTCCCCGCC**

PFKFB3 KO6 allele-2 **CCCCC**^{23bps insertion, 3 bps deletion}**ACCG**_{gcatcatgccttctattt}**gt**-----**TCGTCATGGTGG**

PFKFB3 genome **CCCCC****ACCG**.....**TCATCGTCATGGTGG**

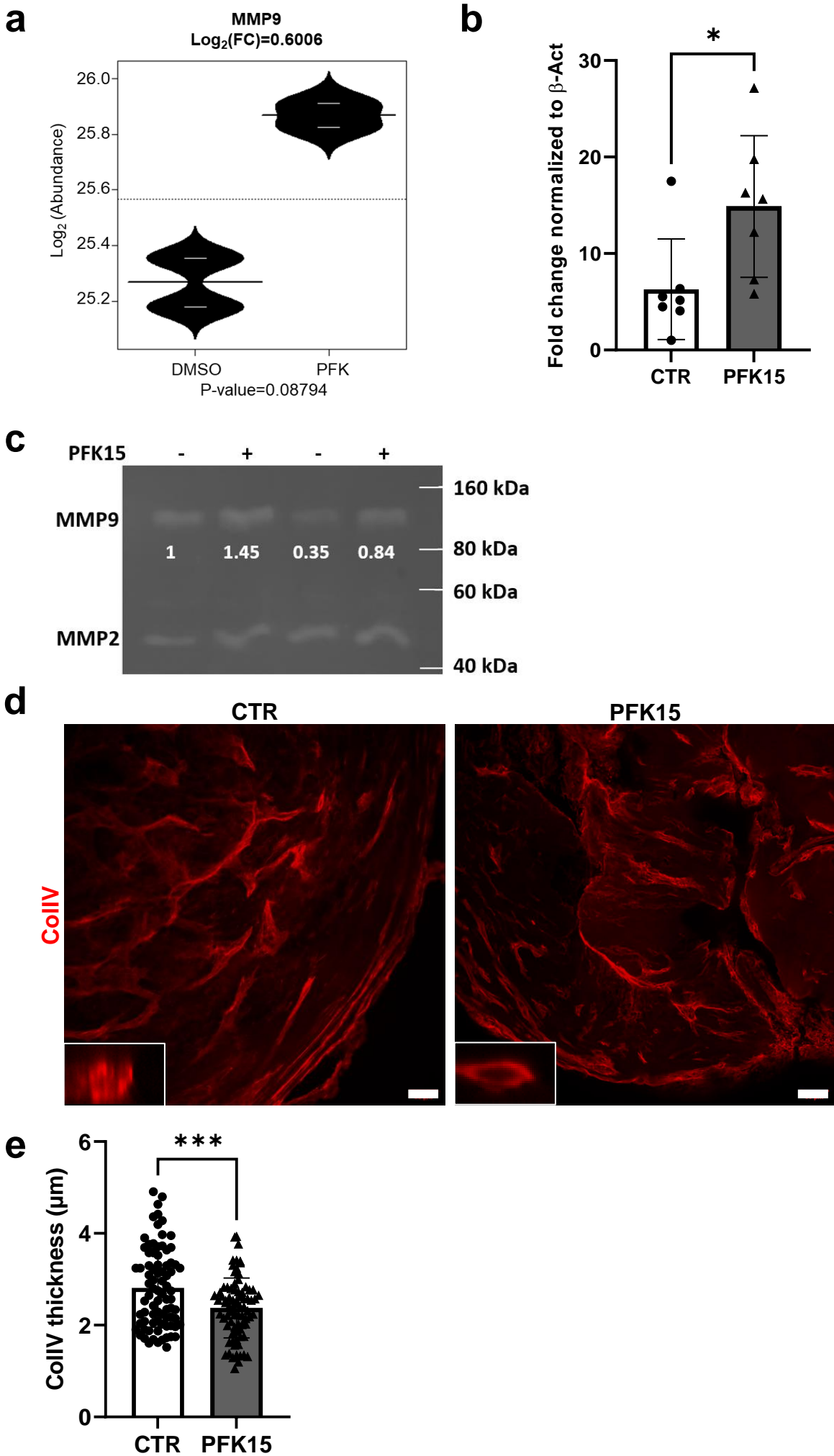
PFKFB3 KO8 allele-1 **CCCCC**^{12bps deletion}**ACCGT**-----**GGGCCTCCCCGCC**

PFKFB3 genome **CCCCC****ACCGTCATCGTCATGGTGGGCCTCCCCGCC**

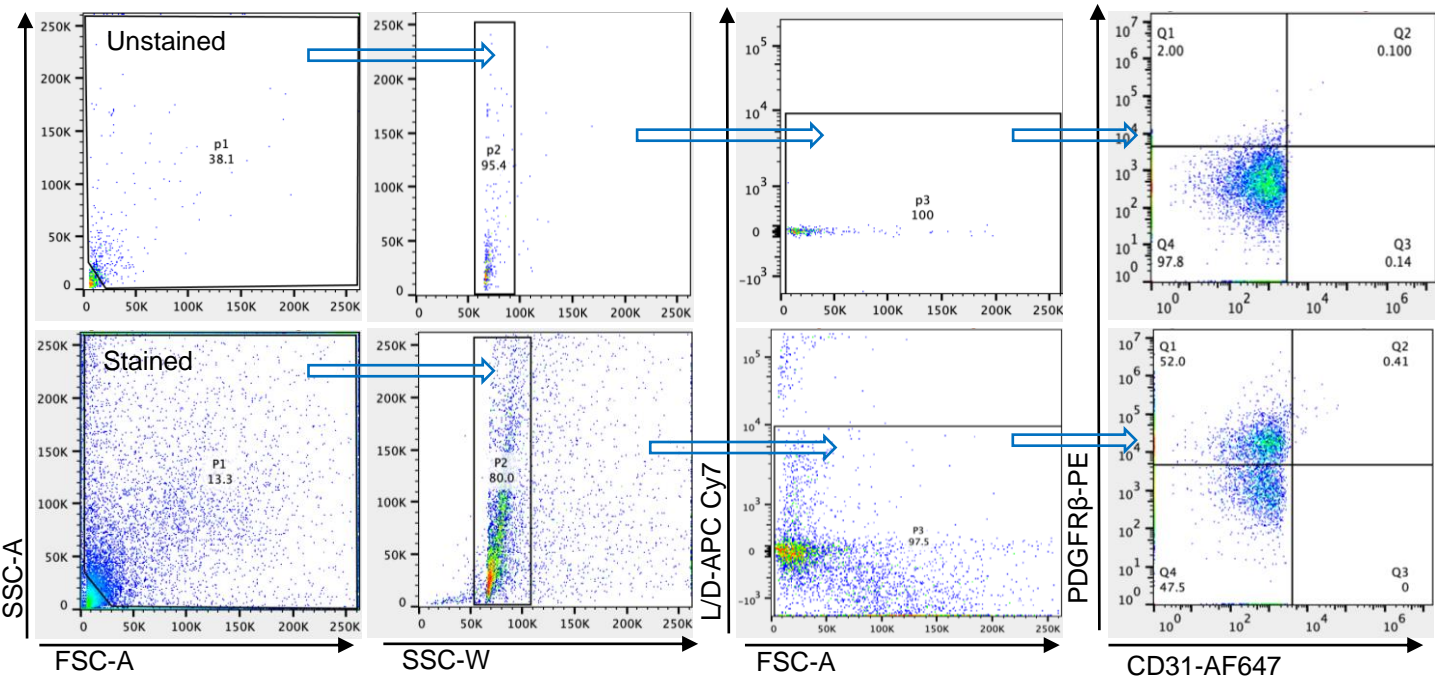
PFKFB3 KO8 allele-2 **CCCCC**^{6 bps deletion}**CA**-----**TCGTCATGGTGGGCCTCCCCGCC**

PFKFB3 genome **CCCCC****ACCGTCATCGTCATGGTGGGCCTCCCCGCC**

Supplementary Figure 6. Generation of *PFKFB3* knockout iPS lines. (a) CRISPR/Cas9 genome editing was used to generate *PFKFB3* knockout iPS lines that lacked the expression of PFKFB3, as determined by western blot analysis. **(b)** Sanger sequencing of genomic DNA revealed the presence of indels in KO6 clone (referred to herein as P206) and deletions in KO8 clone (referred to herein as P208). The PAM sequence is highlighted in bold, insertions are shown in blue and deletions are noted in red.



Supplementary Figure 7. Proteomic analysis of the BVO secretome (a) Differential expression of MMP9 in the BVO secretome as detected by proteomics, n=5 BVOs per pooled sample, 2 separate preparations. Statistical comparison was conducted using the Ebayes method of the limma package. Nominal p-value is displayed in beanplot while corrected for multiple testing p-value with the Benjamini-Hochberg method is provided in Supplemental Data 2. (b) MMP9 gene expression as assessed by qPCR, β -actin was used as a normalization control. n=7 BVOs per group, 3 separate preparations. Data are shown as mean \pm SD. P values were calculated using a two-tailed Student's t-test. (*p=0.0270). (c) Enzymatic activity of gelatinases in the conditioned media of BVOs treated with DMSO (CTR) or PFK15 (2.5 μ M) for 24h, as assessed by zymography. n=5 BVOs per pooled sample, 2 separate preparations. Data were quantified using the ImageJ and normalised to total protein content, as measured by total spectra. (d) Deposition of CollIV in BVOs following PFK15 treatment. Representative images of basement membrane, as detected by immunofluorescence confocal imaging for CollIV in sections from BVOs treated with DMSO (CTR) or PFK15 (2.5 μ M) 24h. Bar scales 50 μ m. (e) Vessel cross-sections were used to quantify basement membrane thickening. N=80 cross-sections in single BVOs from 2 separate preparations per group. Values are presented as mean \pm SD; P values were calculated using a two-tailed Student's t-test. (***)p=0.0004).



Supplementary Figure 8. FACS gating strategy. Gating strategy to determine cell percentage composition of BVOs in Figure 1e.

Supplementary Table S1

Antibodies used for Immunofluorescence staining

Primary antibody	Company Reference	Dilution IMF
CD31	R&D System AF806	1:100
PDGFR β	Cell Signaling #3169	1:100
Collagen IV	Millipore AB769	1:200
Oct4	Thermo TA500035	1:100
Nanog	Sigma N3038	1:100
CD144 (VE-cadherin)	Millipore MABT134	1:200
ZO1	Santacruz Technologies sc-8147	1:100
PDGFR α	Abcam ab203491	1:1000
YAP1	NOVUS NB110-58358	1:500
NG2	Abcam ab86067	1:100
Ki67	Cell Signaling #9129S	1:100
CC3 (Cleaved-Caspase 3)	Cell Signaling #9661S	1:250

Secondary antibody	Company Reference	Dilution IMF
Alexa-Fluor 488 Donkey anti-Sheep	Invitrogen A11015	1:250
Alexa-Fluor 488 Donkey anti-Mouse	Invitrogen A21202	1:250
Alexa-Fluor 488 Donkey anti-Rabbit	Invitrogen A21206	1:250
Alexa-Fluor 555 Donkey anti-Rabbit	Invitrogen A31572	1:250
Alexa-Fluor 633 Donkey anti-Mouse	Invitrogen A21100	1:250
Alexa-Fluor 647 Donkey anti-Rabbit	Invitrogen A31573	1:250
Alexa-Fluor 647 Donkey anti-Goat	Jackson Immunolabs 705-606-147	1:250

Supplementary Table S2

Primary antibody	Company Reference	Dilution
CD31-AlexaFluor647	BD Biosciences, 558094	5 μ l/test
CD140b-PE	BD Biosciences, 558821	20 μ l/test
CD144-FITC	BD Biosciences, 560874	20 μ l/test
CD45-FITC	Invitrogen, 11-0459-41	5 μ l(0.25 μ g)/test
CD90-PerCP/Cyanine5.5	Biolegend, 328117	1 μ g/million cells
CD73-BV650	BD Biosciences, 742633	10 μ l/test
CD44-PE	BD Biosciences, 550989	20 μ l/test
CD144-BV786	BD Biosciences, 565672	5 μ l(0.25 μ g)/test
Live/Dead-FVS780	BD Biosciences, 565388	0.1 μ l/test

Supplementary Table S3

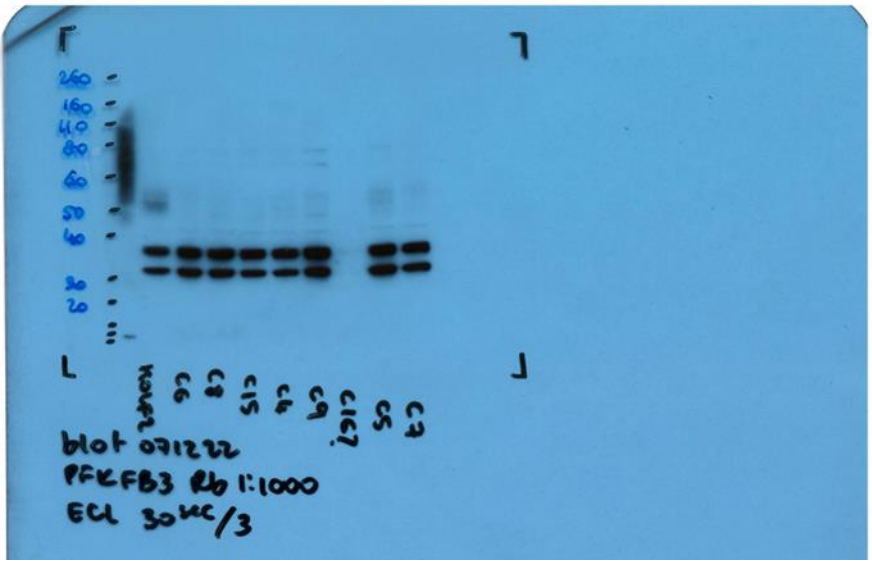
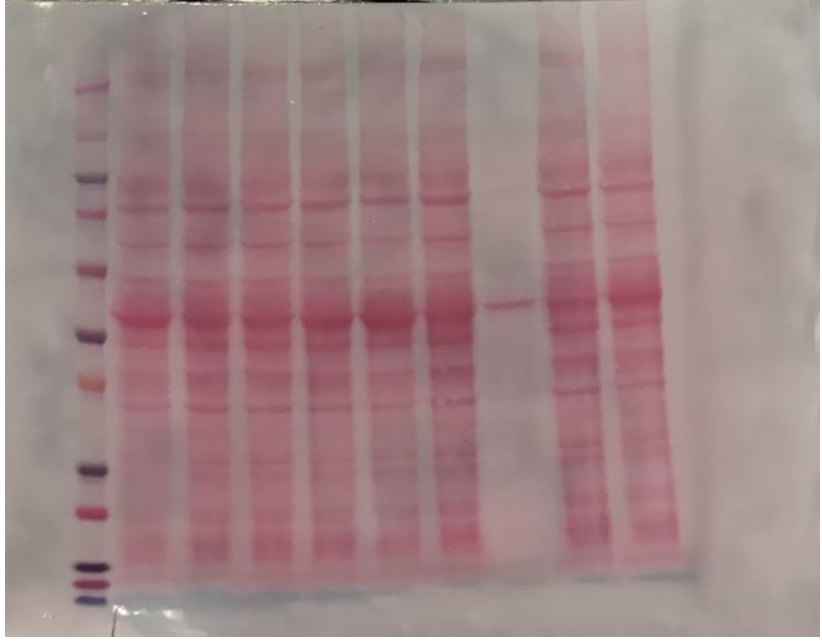
List of antibodies used for Western blot Analysis

Primary antibody	Company Reference	Dilution WB
CD31	Abcam ab28364	1:500
CD144 (VE-cadherin)	Millipore MABT134	1:2000
KDR (VEGFR2)	Cell Signaling #2479	1:1000
eNOS	BD Biosciences 610297	1:5000
Oct4	Thermo TA500035	1:1000
GAPDH	Santacruz Technologies sc-25778	1:1000
Histone H3 (H-H3)	Cell Signaling #9715S	1:1000
YAP1	NOVUS NB110-58358	1:500

Secondary antibody	Company Reference	Dilution WB
Peroxidase AffiniPure Goat Anti-Mouse IgG	Jackson Immunolabs 115-035-174	1:4000
Peroxidase IgG Fraction Monoclonal Mouse Anti-Rabbit IgG	Jackson Immunolabs 211-032-171	1:4000

Source Data file

Uncropped image of panel Supplementary Figure 6a.



Source Data file

Uncropped image of panel Supplementary Figure 7c.

